ACKNOWLEDGMENTS

We wish to express our gratitude to the members of group F 41 of DESY for their hospitality and to R. R. I. Zucca and Y. R. Shen for making available to us their results prior to publication. On of us (P. Y. Y.) is indebted to General Telephone and Electronics for a Fellowship. We are also grateful to Dr. J. C. Phillips and Dr. J. A. Van Vechten for valuable discussions and for sending us preprints of their work.

[1]J. C. Phillips, Phys. Rev. Letters 20, 550 (1968); *Covalent Bonding in Crystals, Molecules, and Polymers* (University of Chicago Press, Chicago, 1969).

[2]J. C. Phillips and J. A. Van Vechten, Phys. Rev. Letters 22, 705 (1969).

[3]J. C. Phillips, Phys. Rev. Letters 22, 645 (1969).

[4]J. C. Phillips and J. A. Van Vechten, Phys. Rev. 183, 709 (1969).

[5]B. F. Levine, Phys. Rev. Letters 22, 787 (1969).

[6]J. A. Van Vechten, M. Cardona, D. E. Aspnes, and R. M. Martin, Proceedings of the International Conference of the Physics of Semiconductors, Cambridge, Mass., 1970 (unpublished).

[7]D. Penn, Phys. Rev. 128, 2093 (1962).

[8]V. Heine and R. O. Jones, J. Phys. C 2, 719 (1969).

[9]J. A. Van Vechten, Phys. Rev. 182, 891 (1969).

[10]M. Cardona, J. Appl. Phys. 36, 2181 (1965).

[11]In Ref. 8 Heine and Jones calculated the band gap at X both by perturbation theory and also more exactly by diagonalisation of a 6×6 matrix. They found that the perturbation theory gave better agreement with experiment than the more exact method. We found that this is also true for the III-V compounds. As a result we have used the expressions obtained by perturbation theory.

[12]C. Keffer, T. M. Hayes, and A. Bienenstock, Phys. Rev. Letters 21, 1676 (1968).

[13]J. P. Walter, R. R. L. Zucca, M. L. Cohen, and Y. R. Shen (unpublished).

[14]A. A. Maradudin, E. W. Montroll, and G. H. Weiss, in *Solid State Physics*, edited by F. Seitz and D. Turnbull (Academic Press, New York, 1963), Suppl. 3, p. 237.

[15]G. C. Benson and E. K. Gill, Can. J. Phys. 44, 614 (1966).

[16]W. J. L. Buyers and T. Smith, J. Phys. Chem. Solids 29, 105 (1968).

[17]B. W. Batterman and D. R. Chipman, Phys. Rev. 127 690 (1962).

[18]J. C. Phillips, Rev. Mod. Phys. 42, 317 (1970).

PHYSICAL REVIEW B VOLUME 2, NUMBER 8 15 OCTOBER 1970

Band Structure of SiGe: Coherent-Potential Approximation*

D. Stroud† and H. Ehrenreich

Division of Engineering and Applied Physics, Harvard University, Cambridge, Massachusetts 02138

(Received 4 March 1970)

The band structure of SiGe has been calculated using the coherent-potential approximation in conjunction with a realistic but local pseudopotential model. The effects of alloy disorder manifest themselves in complex band energies, each with an imaginary part inversely proportional to the electron lifetime. Spectral functions and the alloy denisty of states are also computed. The damping proves to be small, though it is not always given accurately by low-order-perturbation theory about the virtual crystal. Moreover, within the present local pseudopotential approximation, it affects only s electrons capable of penetrating the ionic cores, since outside the core region the alloy pseudopotential is like that of either limiting pure crystal. The effect of the damping on experimental quantities such as the optical absorption and electrical resistivity is very small.

I. INTRODUCTION

This paper describes a calculation of the band structure of SiGe, in which we explicitly include the effects of alloy disorder. These manifest themselves in complex band energies with imaginary parts inversely proportional to the electron lifetime. Such a calculation has been made feasible, and potentially useful, by the development of the so-called coherent-potential approximation (CPA) by Soven,[1] Taylor,[2] Onodera and Toyozawa,[3] and Velický, Kirkpatrick, and Ehrenreich.[4] The CPA is a method for treating the single-particle properties of substitutionally disordered binary alloys within the framework of multiple-scattering theory. It consists of approximating the configuration-averaged single-particle alloy Green's function $\langle G \rangle$ by an operator $\overline{G}$ determined by the condition that an electron propagating according to it should undergo, on the average, no scattering at each atomic site. The CPA neglects effects due to the clustering of like atoms

in the alloy. Such clustering, which will occur statistically even in alloys with no short-range order, is likely to be significant whenever the constituent atoms have very different scattering strengths. However, as has been shown by Velický *et al.*,[4] the CPA should be an excellent approximation at all concentrations in alloys where the atomic characteristics are not too different.

A natural starting point for applying the CPA to a binary alloy is the one-electron Hamiltonian H in Wannier representation. The general multiband situation is difficult to treat calculationally. A model Hamiltonian with random diagonal and periodic off-diagonal elements has, however, been used for studying both the single-band[4,5] and degenerate tight-binding[6] cases. The latter model approximates NiCu alloys, for which it gives good results. For such calculations, the one-electron properties of the alloy can be found without knowledge of any $E(k)$ relations. In the nondegenerate case, for example, one requires as inputs only the relative concentrations x and $1-x$ of the two alloy constituents, the difference δ between the two atomic energy levels, and the pure crystal density of states, which is required by the model to be of the same shape for the two limiting pure crystals.

In order to utilize the CPA to obtain complex $E(k)$ curves for alloys, we require a more general model Hamiltonian. Since orthogonalized-plane-wave (OPW) and pseudopotential methods have been so useful in band calculations for pure crystals, and since in alloys they would be expected to be best for the same weak-scattering systems for which the CPA itself is most accurate, these techniques will be suitably generalized in Sec. II to apply to binary alloys. Because of the multiple-scattering nature of the CPA, the method is compatible with it only if the random part of alloy Hamiltonian is composed of cell-localized random contributions from each atom. Ideally, one wants to deal with a binary alloy of isoelectronic constituents whose potentials in the perfect crystal differ only in the core regions. Then the alloy potential outside the core region will be like that of either limiting perfect crystal, and only electrons able to penetrate core regions will experience alloying effects.

SiGe is an almost ideal example of the kind of behavior just discussed and will be considered here for that reason. A model Hamiltonian suitable for that alloy is described in Sec. II. To exhibit its features in the most transparent form, the derivation is then carried out for a Bravais lattice. The necessary generalization to the diamond lattice is made in Sec. III. Since this is straightforward, the discussion is mostly confined to a statement of formal results.

After a brief description of calculational approximations, and an outline of the numerical procedures necessary to solve the equations,[7] the electronic density of states, self-energy functions, spectral densities, and complex $E(k)$ curves for SiGe are presented in Sec. IV. Since the present work supports the long-held view[8-10] that the virtual-crystal model should be very good for SiGe alloys, the results reveal relatively little that will be surprising physically. However, the present work is believed to represent the first approximate calculation of the "complex band structure" of a semiconductor alloy using a suitably generalized OPW method and, as such, clearly exhibits the kind of detailed information to be expected from such calculations, as well as the problems involved. One such problem is the necessity of calculating accurately certain matrix elements of Green's functions which involve sums over the Brillouin zone. This is likely to cause considerable numerical difficulties in calculations on systems where the virtual crystal no longer represents a good lowest approximation.

To illustrate the kinds of behavior to be expected when the random alloy potentials are stronger than in SiGe, and when in fact it is no longer desirable to use the virtual crystal as a good lowest approximation, some additional results are also exhibited for hypothetical alloys having the same virtual crystal potential as SiGe, but a greater difference between the atomic potentials.

II. FORMALISM

Consider a substitutional binary alloy A_xB_{1-x} whose constituent atoms are distributed at random on N atomic sites, one per unit cell, and assume that the one-electron Hamiltonian H can be expressed as

$$H = p^2/2m + \sum_l V_l \quad ,$$

where $V_l = V_l^A$ or V_l^B is the random potential associated with the lth site. It will be convenient to write H in terms of the virtual-crystal Hamiltonian

$$H^{\mathrm{vc}} = p^2/2m + \sum_l V_l^{\mathrm{vc}} \, , \quad V_l^{\mathrm{vc}} = x\,V_l^A + (1-x)\,V_l^B \quad .$$

Then H is given by

$$H = H^{\mathrm{vc}} + \sum_l (V_l - V_l^{\mathrm{vc}}) \equiv H^{\mathrm{vc}} + U \equiv H^{\mathrm{vc}} + \sum_l U_l \quad . \tag{2.2}$$

U_l thus represents the deviation of the random potential associated with site l from the virtual-crystal potential.

To treat H within the CPA, we introduce the propagator

$$G(z) = (z - H)^{-1} \tag{2.3}$$

for the random medium. The measurable single-particle properties of H are then determined by the average of G over all possible alloy configurations, namely,

$$\overline{G} \equiv \langle G(z) \rangle = \langle (z - H)^{-1} \rangle \equiv (z - H^{vc} - \Sigma)^{-1} ,$$

$$\Sigma = \sum_l (\Sigma_l) . \qquad (2.4)$$

Equation (2.4) defines the self-energy Σ of the alloy with respect to the virtual crystal. Since G has the full crystal symmetry, so has Σ, whence Σ can be expressed as a sum of atomic contributions Σ_l from each site. $\overline{G}$ and Σ, like other Green's functions and self-energy operators, [11] are analytic in both half-planes and satisfy the relation

$$\overline{G}^{\dagger}(z) = \overline{G}(z^*) \quad , \quad \Sigma^{\dagger}(z) = \Sigma(z^*) \quad .$$

In discussing the physical properties of alloys, we generally shall make use only of the retarded operators G and Σ, i.e., those which are analytic in the upper half-plane.

The scattering of an electron due to deviations of the alloy from its averaged behavior is described by the total T matrix

$$T = U - \Sigma + t(U - \Sigma)\overline{G}T. \qquad (2.5)$$

Expanding G about $\overline{G}$ then yields

$$G = \overline{G} + \overline{G}\,T\,\overline{G} \qquad (2.6)$$

and the exact condition

$$\langle T(z) \rangle = 0 \quad , \qquad (2.7)$$

which defines $\overline{G}$.

The CPA consists of replacing Eq. (2.7) by the approximate relation

$$\langle T_l(z) \rangle = x\, T_l^A(z) + (1 - x)\, T_l^B(z) = 0 \quad , \qquad (2.8)$$

where $T_l^{A,B}(z)$ is the atomic T matrix associated with an A or B atom at site l:

$$T_l^{A,B} = U_l^{A,B} - \Sigma_l + (U_l^{A,B} - \Sigma_l)\overline{G}\,T_l^{A,B} . \qquad (2.9)$$

Substitution of (2.9) into (2.8) yields the operator equation

$$\Sigma_l = (x\,\Delta_l - \Sigma_l)\,\overline{G}\,(y\,\Delta_l + \Sigma_l) \quad , \qquad (2.10)$$

where $y = 1 - x$ and $\Delta_l = U_l^B - U_l^A$ is the difference between the two random potentials at site l.

Equation (2.10) is a self-consistency condition which determines Σ within the CPA. Together with Eq. (2.4), it may be solved to obtain the CPA for Σ and $\overline{G}$. As is evident from (2.8), an electron propagating according to the $\overline{G}$ thus determined will undergo, on the average, no further scattering at each atomic site in the lattice. It may be shown that approximating the exact $\langle G \rangle$ by this $\overline{G}$ is in fact equivalent to assuming that the T matrix associated with a given atom is statistically uncorrelated with an incident electron wave made up of contributions previously scattered off all other atoms. [4]

All the one-electron properties of the alloy can be expressed in terms of $\overline{G}$ and Σ. The spectral function $A(\vec{k}, E)$, representing the probability per unit energy that an electron having Bloch wave number $\vec{k}$ has energy E, may be written as

$$A(\vec{k}, E) = -\pi^{-1} \sum_n \langle n\vec{k} |\, \overline{G}(E + i0)\, | n\vec{k} \rangle \quad , \qquad (2.11)$$

where $|n\vec{k}\rangle$ denotes an eigenstate of H^{vc} having wave number $\vec{k}$ and band index n. In a pure crystal, $A(\vec{k}, E)$ will consist of a series of δ-function spikes, but in the alloy these will be broadened. The total density of states per atom is

$$\rho(E) = N^{-1} \sum_{\vec{k}} A(\vec{k}, E)$$

$$= -(N\pi)^{-1}\, \mathrm{Im} \sum_{n\vec{k}} \langle n\vec{k} |\, \overline{G}(E + i0)\, | n\vec{k} \rangle . \qquad (2.12)$$

The "complex band structure" of the alloy may be obtained by finding the poles of the (retarded) Green's function $\overline{G}$ in the lower half-plane by analytic continuation, or equivalently, by diagonalizing the "effective Hamiltonian" $H_{\mathrm{eff}} = H^{vc} + \Sigma$. H_{eff} is periodic but non-Hermitian. Its eigenstates are therefore Bloch waves but its eigenvalues are complex. If a spectral peak is Lorentzian, its half-width will be given by twice the imaginary part of the corresponding eigenvalue.

We wish to apply the CPA to an alloy described by a pseudopotential model. To that end, we introduce a pseudo-Hamiltonian of the form [12]

$$H_p = (1 - P)H \quad , \qquad (2.13)$$

where

$$P = \sum_l \sum_c \gamma_{cl} |cl\rangle\langle cl| \equiv \sum_l P_l \qquad (2.14)$$

projects out that portion of H which can be expanded as a linear combination of core states $|cl\rangle$ associated with atomic orbitals c at site l. Since the core states in general are different for the two types of atoms in the alloy, the P_l's are random operators.

Just as in pure crystals, H_p gives the same spectrum of valence eigenvalues as H (though not the same wave functions) for any alloy configuration, and for arbitrary complex coefficients γ_{cl}, which may then be chosen so as to minimize the random parts of H_p. Thus, since the poles of G and $G_p = (z - H_p)^{-1}$ are the same, so are those of $\langle G \rangle$ and $\langle G_p \rangle$. Since the random pseudopotentials appearing in H_p are smaller than those in H, the CPA will be more accurate for the former, and the poles of $\overline{G}_p$ will more closely approximate those of $\langle G \rangle$ than will the poles of $\overline{G}$. In order to insure that $\overline{G}_p$ yields the same density of states and spectral functions as $\overline{G}$, we shall assume [13] that H_p is energy independent.

To apply the CPA to H_p, the random parts of H_p must be expressible as a sum of random parts from each site, as in (2.2). To see when this is possible, we use the fact that the kinetic energy is not affect-

ed by P, and write

$$H_p = p^2/2m + (1 - \sum_l P_l)\sum_{l'} V_{l'} \quad . \tag{2.15}$$

Introducing the pseudo-Hamiltonians

$$H_p^{A,B} = p^2/2m + (1 - \sum_l P_l^{A,B})\sum_{l'} V_{l'}^{A,B} \tag{2.16}$$

of the two limiting pure crystals, we write H_p as

$$H_p = H_p^{vc} + (H_p - H_p^{vc}) \quad , \tag{2.17}$$

where

$$H_p^{vc} = x H_p^A + (1-x) H_p^B \quad . \tag{2.18}$$

The first term of (2.17) is periodic. The second term can be reduced, with the help of Eqs. (2.15), (2.16), and (2.18), to

$$H_p - H_p^{vc} = \sum_l U_l^p - \sum_{l \neq l'} \sum P_l (V_{l'} - V_l^{vc}) \quad , \tag{2.19}$$

where

$$U_l^p = (1 - P_l)(V_l - V_l^{vc}) - P_l V^{vc} + x P_l^A V^A + (1-x) P_l^B V^B \quad , \tag{2.20}$$

with

$$V^{vc} = \sum_l V_l^{vc} \; ; \quad V^{A,B} = \sum_l V_l^{A,B} \quad .$$

Thus, H_p can be written in the desired form provided the double sum in (2.19) is negligible. This will be so if V_l^B and V_l^A are the same outside the lth atomic cell, i.e., if $V_l^B - V_l^A$ is cell localized. Such a condition is expected to be valid in an alloy like SiGe of two isoelectronic elements, but is less likely when the two constituents are of different valence.

U_l^p would be difficult to calculate explicitly from Eq. (2.20). But when the double sum can be neglected,

$$H_p^{A,B} = H_p^{vc} + \sum_l (U_l^p)^{A,B} \tag{2.21}$$

and the U_l^p's may be obtained directly from the pseudopotentials of the limiting pure crystals.

In order to make the solution of Eq. (2.10) tractable in a multiband situation, where it would in general be a matrix equation, we make the following ansatz for the form of Δ_l:

$$\Delta_l = \delta \, |wl\rangle \langle wl| \quad . \tag{2.22}$$

Here, $|wl\rangle$ is a member of some complete set of basis functions associated with site l. $|wl\rangle$ is assumed to be essentially localized within the atomic cell but is not directly connected to any Wannier function of the alloy Hamiltonian. This function is introduced simply as a means of representing the difference between the atomic pseudopotentials in SiGe. It should be noted, however, that the model is not necessarily restricted to pseudopotential applications.

If Δ_l is given by (2.22), Σ_l must be of the same form:

$$\Sigma_l = g(z) \, |wl\rangle \langle wl| \quad . \tag{2.23}$$

Thus, Eq. (2.10) becomes

$$g(z) = [x\delta - g(z)] F(z) [y\delta + g(z)] \quad , \tag{2.24}$$

where

$$F(z) = \langle wl | \, \overline{G}(z) \, | wl \rangle \quad . \tag{2.25}$$

Equation (2.24) is an algebraic equation. To solve it, we need an expression for $F(z)$. Because of the weakness of the random scatterers in SiGe, it is convenient to express this quantity in terms of matrix elements of $G^{vc}(z) = (z - H^{vc})^{-1}$. We therefore introduce the operators

$$\overline{G}_{\vec{k}} = \sum_{nn'} |n\vec{k}\rangle \langle n\vec{k}| (z - H^{vc} - \Sigma)^{-1} |n'\vec{k}\rangle \langle n'\vec{k}| \tag{2.26}$$

and

$$G_{\vec{k}}^{vc} = \sum_n (z - E_{n\vec{k}})^{-1} |n\vec{k}\rangle \langle n\vec{k}| \quad , \tag{2.27}$$

where $E_{n\vec{k}}$ is the eigenvalue corresponding to virtual-crystal state $|n\vec{k}\rangle$. Equation (2.26) recognizes that in general H_{eff} is not diagonal in n. Using the fact that $\overline{G}$, G^{vc}, and Σ are all diagonal in $\vec{k}$, we may then write the Dyson equation

$$\overline{G} = G^{vc} + G^{vc} \Sigma \, \overline{G} \tag{2.28}$$

as the N equations

$$\overline{G}_{\vec{k}} = G_{\vec{k}}^{vc} + G_{\vec{k}}^{vc} \; \Sigma \, \overline{G}_{\vec{k}} \quad . \tag{2.29}$$

Since Σ can be expressed in terms of the basis functions $|wl\rangle$ by means of (2.23), Eq. (2.29) is readily solved. We find that

$$F(z) = N^{-1} \sum_{\vec{k}} F(\vec{k}, z) = N^{-1} \sum_{\vec{k}} \frac{F_0(\vec{k}, z)}{1 - g(z) F_0(\vec{k}, z)} \quad , \tag{2.30}$$

where

$$F(\vec{k}, z) = N \langle wl | \, \overline{G}_{\vec{k}} \, | wl \rangle \quad , \tag{2.31}$$

$$F_0(\vec{k}, z) = N \langle wl | \, G_{\vec{k}}^{vc} \, | wl \rangle = \sum_n f_{n\vec{k}} (z - E_{n\vec{k}})^{-1} \quad , \tag{2.32}$$

and

$$f_{n\vec{k}} = N |\langle wl | n\vec{k} \rangle|^2 \quad .$$

Note that, since the alloy potential does not flip spins, the sums in the expressions just given are *not* to be taken over spin.

The physical significance of $F(z)$ is that

$$-\pi^{-1} \operatorname{Im} F(E^+) = \rho^w(E) \tag{2.33}$$

is the density of states for electrons whose eigen-

states are projected into orbital $|wl\rangle$, i.e., in the spatial region where random potential is appreciable. Since ρ^w is like a spectral density, it satisfies the sum rule

$$\int_{-\infty}^{\infty} \rho^w(E)\,dE = 1 \quad . \tag{2.34}$$

To find the alloy density of states, we must evaluate Eq. (2.12). For this, and also to calculate the self-energy $\Sigma_{n\vec{k}}$ of an electron in virtual-crystal state $|n\vec{k}\rangle$, an explicit expression for the diagonal matrix element $\langle n\vec{k}|\,\overline{G}\,|n\vec{k}\rangle$ will be needed. Using (2.29), one obtains

$$\begin{aligned}\langle n\vec{k}|\,\overline{G}(z)\,|n\vec{k}\rangle &= (z-E_{n\vec{k}})^{-1} + g(z) f_{n\vec{k}} (z-E_{n\vec{k}})^{-2} \\ &\quad \times [1 - g(z) F_0(\vec{k}, z)]^{-1} \\ &\equiv [z - E_{n\vec{k}} - \Sigma_{n\vec{k}}(z)]^{-1} \quad ,\end{aligned} \tag{2.35}$$

which defines $\Sigma_{n\vec{k}}(z)$. After some rearrangement, $\Sigma_{n\vec{k}}$ is seen to be

$$\Sigma_{n\vec{k}}(z) = g(z) f_{n\vec{k}} \Big/ \left[1 - g(z) \sum_{n' \neq n} \frac{f_{n'\vec{k}}}{z - E_{n'\vec{k}}}\right] \quad . \tag{2.36}$$

Equation (2.36) corresponds to the self-consistent CPA solution for the self-energy if $g(z)$ is determined from (2.24). This latter equation may be solved in principle, because substitution of (2.30) into it yields a form involving $g(z)$ as the only unknown function.

Using (2.35) and (2.12), one finds that for the density of states

$$\begin{aligned}\rho(E) &= \rho_{vc}(E) - (N\pi)^{-1} \\ &\quad \times \frac{\partial}{\partial E} \sum_{\vec{k}} \arg[1 - g F_0(\vec{k}, E)]\big|_{g=g(E)} \quad ,\end{aligned} \tag{2.37}$$

where ρ_{vc} is the density of states in the virtual crystal. Equation (2.37) exhibits a strong formal similarity to an expression derived by Izyumov[14] for the density of states of an alloy in the low-concentration limit. But the dependence of the strength g of the effective random potential upon energy makes the coherent-potential expression much more difficult to use in numerical applications.

Similarly, the spectral function [Eq. (2.11)] is

$$\begin{aligned}A(\vec{k}, E) &= A_{vc}(\vec{k}, E) - \pi^{-1} \\ &\quad \times \frac{\partial}{\partial E} \arg[1 - g F_0(\vec{k}, E)]\big|_{g=g(E)} \quad .\end{aligned} \tag{2.38}$$

Equations (2.35) and (2.36) show that the poles of $\overline{G}$ occur when

$$1 - g(z) F_0(\vec{k}, z) = 0. \tag{2.39}$$

These determine the complex $E(\vec{k})$ spectrum for the alloy. Alternatively, one may obtain the poles by solving the equation

$$\det[z - H_{\text{eff}}(z)] = 0. \tag{2.40}$$

III. GENERALIZATION TO THE DIAMOND LATTICE

The diamond lattice has two atoms per unit cell. Without loss of generality, these may be chosen to be located at $\vec{R}_l \pm \frac{1}{2}\vec{b}$, where $\vec{R}_l$ is the position vector for the lth unit cell. The formalism presented in the previous section may be simply generalized. While an equation of the form (2.24) will still apply in a complex lattice, $F(z)$ can no longer be written in the simple form (2.30). One obtains, instead, matrix equations involving site indices μ, μ' of different atoms within the unit cell:

$$\begin{aligned}F_{\mu\mu'}(\vec{k}, z) &= F^0_{\mu\mu'}(\vec{k}, z) + n_b^{-1}\, g(z) \\ &\quad \times \sum_{\mu''} F^0_{\mu\mu''}(\vec{k}, z) F^0_{\mu''\mu'}(\vec{k}, z) \quad ,\end{aligned} \tag{3.1}$$

with n_b the number of atoms per unit cell and

$$F_{\mu\mu'}(\vec{k}, z) = N\langle wl\mu\,|\,\overline{G}_{\vec{k}}\,|wl\mu'\rangle \quad , \tag{3.2}$$

$$F^0_{\mu\mu'}(\vec{k}, z) = N\langle wl\mu\,|\,G^{vc}_{\vec{k}}\,|wl\mu'\rangle \tag{3.3}$$

replacing Eqs. (2.31) and (2.32). For the diamond lattice, (3.1) is a 2×2 matrix equation which may easily be solved.

Since pseudopotential coefficients in OPW schemes for pure crystals are commonly specified by the values of their Fourier components at reciprocal-lattice vectors $\vec{K}$, it is convenient to specify the random deviations U_l and solutions to (3.1) similarly. The matrix elements of Δ_l that will appear in the CPA are diagonal in Bloch index $\vec{k}$ and off-diagonal in $\vec{K}$. According to (2.22) they are given by

$$\begin{aligned}\langle \vec{k}+\vec{K}\,|\,\Delta_l\,|\vec{k}+\vec{K}'\rangle &= \delta\,\langle \vec{k}+\vec{K}\,|wl\rangle\langle wl\,|\vec{k}+\vec{K}'\rangle \\ &= N^{-1}\delta\, e^{-i(\vec{K}-\vec{K}')\cdot b/2}\,\phi(\vec{k}+\vec{K})\,\phi(\vec{k}+\vec{K}') \quad ,\end{aligned} \tag{3.4}$$

with

$$\phi(\vec{k}+\vec{K}) = N^{1/2}\langle \vec{k}+\vec{K}\,|w0\rangle \quad .$$

For the properties of physical interest, we shall need to know only $F_{++}(\vec{k}, z) = F_{--}(\vec{k}, z)$, where + and − refer, respectively, to the basic sites $+\frac{1}{2}b$ and $-\frac{1}{2}$b, because

$$F(z) = N^{-1} \sum_{\vec{k}} F_{++}(\vec{k}, z) \quad . \tag{3.5}$$

Solving (3.1), one finds that

$$F_{++}(\vec{k}, z) = -\frac{\partial}{\partial g} \ln[1 - g Q_1(\vec{k}, z) + g^2 Q_2(\vec{k}, z)]\Big|_{g=g(z)} \quad , \tag{3.6}$$

with

$$\begin{aligned}Q_1 &= F^0_{++}(\vec{k}, z) = F^0_{CC} + F^0_{SS} \quad , \\ Q_2 &= F^0_{CC} F^0_{SS} - F^0_{CS} F^0_{SC} \quad ,\end{aligned}$$

and

$$F^0_{CC}(\vec{k},z)=\sum_n f^C_{n\vec{k}}(z-E_{n\vec{k}})^{-1}\,,$$

$$F^0_{SS}(\vec{k},z)=\sum_n f^S_{n\vec{k}}(z-E_{n\vec{k}})^{-1}\,, \tag{3.7}$$

$$F^0_{CS}(\vec{k},z)=F^0_{SC}(\vec{k},z)=\sum_n (f^C_{n\vec{k}}f^S_{n\vec{k}})^{1/2}(z-E_{n\vec{k}})^{-1}\,,$$

$$f^C_{n\vec{k}}=\sum_{\vec{K}}\phi(\vec{k}+\vec{K})\,a_{n\vec{K}}(\vec{k})\cos\tfrac{1}{2}\vec{K}\cdot\vec{b}\,,$$

$$f^S_{n\vec{k}}=\sum_{\vec{K}}\phi(\vec{k}+\vec{K})\,a_{n\vec{K}}(\vec{k})\sin\tfrac{1}{2}\vec{K}\cdot\vec{b}\,.$$

Here $a_{n\vec{K}}(\vec{k})=\langle\vec{k}+\vec{K}|n\vec{k}\rangle$ is a coefficient in the expansion of $|n\vec{k}\rangle$ in plane waves.

The electronic properties discussed in the preceding section are easily generalized to an alloy having the diamond structure. The spectral function and density of states are, respectively,

$$A(\vec{k},E)=A_{vc}(\vec{k},E)-\pi^{-1}\times\frac{\partial}{\partial E}\arg[1-gQ_1(\vec{k},E^+)+g^2Q_2(\vec{k},E^+)]\Big|_{g=g(E^+)} \tag{3.8}$$

and

$$\rho(E)=N^{-1}\textstyle\sum_{\vec{k}}A(\vec{k},E)\,. \tag{3.9}$$

The complex eigenvalues are determined by the condition

$$1-g(z)\,Q_1(\vec{k},z)+g^2(z)Q_2(\vec{k},z)=0\,. \tag{3.10}$$

IV. APPLICATION TO SiGe

The band structures of pure Si and Ge are well calculated by a local and energy-independent pseudopotential approximation originally proposed by Brust,[15] according to which all pseudopotential coefficients are neglected except those corresponding to the [111], [220], and [311] components. For the diamond structure in general, one can write

$$\langle\vec{k}+\vec{K}|\,V\,|\vec{k}'+\vec{K}'\rangle=\delta_{\vec{k}\vec{k}'}\,V_{\vec{K}-\vec{K}'}\cos\tfrac{1}{2}(\vec{K}-\vec{K}')\cdot\vec{b}\,. \tag{4.1}$$

In the Brust scheme V_{111}, V_{220}, and V_{311} are given for Si and Ge by -0.21, $+0.04$, $+0.08$ Ry, and -0.23, $+0.01$, $+0.06$ Ry, respectively.

The difference between the Si and Ge form factors, thus, is evidently almost a constant for all three sets of reciprocal-lattice vectors. If this constancy persisted to arbitrarily large $|\vec{K}-\vec{K}'|$, the spatial difference between the Si and Ge atomic pseudopotentials would amount to a δ function at the nucleus, thus trivially satisfying the separability condition (2.22). We shall, therefore, construct a model potential for SiGe alloys which satisfies (2.22) and is such that the Fourier components $\phi(\vec{k}+\vec{K})=\langle\vec{k}+\vec{K}|w0\rangle$ are *constant* out to some maximum wave number $|\vec{k}+\vec{K}|=k_{max}$, and zero thereafter. δ will be chosen so that the *average of the difference* between the three Brust coefficients is reproduced for all $|\vec{k}+\vec{K}|$ and $|\vec{k}+\vec{K}'|<k_{max}$. k_{max} should be between $2\pi\sqrt{(11)}/a$ and $2\pi\sqrt{(16)}/a$, where a is the fcc cube edge; we choose it arbitrarily to be $2\pi\sqrt{(12)}/a$. Then Δ_l is given by Eq. (3.4), with

$$\phi(\vec{k}+\vec{K})=\phi_0,\quad |\vec{k}+\vec{K}|\le(2\pi/a),\sqrt{12}$$
$$=0,\quad\text{otherwise}\,. \tag{4.2}$$

ϕ_0 is determined by the completeness condition

$$\sum_{\vec{k}\vec{K}}\left|\phi(\vec{k}+\vec{K})\right|^2=\frac{\Omega}{8\pi^3}\phi_0^2\int_{|\vec{q}|\le 2\pi\sqrt{(12)}/a}d^3q=N\,,$$

where Ω is the crystal volume, and turns out to be

$$\phi_0=0.21\,. \tag{4.3}$$

δ is given by

$$\delta\phi_0^2=\tfrac{1}{3}(V^{Si}_{111}+V^{Si}_{220}+V^{Si}_{311}-V^{Ge}_{111}-V^{Ge}_{220}-V^{Ge}_{311})$$
$$=0.023\text{ Ry}\,. \tag{4.4}$$

We complete the specification of the model Hamiltonian by requiring that the virtual-crystal pseudopotential $\langle V\rangle=xV^{Si}+(1-x)V^{Ge}$ equal that derived from the Brust form factors at a concentration of 37 at.% Si. This concentration is chosen because concentrations very much nearer $Si_{0.50}$ $Ge_{0.50}$ appear to be rather difficult to work with experimentally.[16] The alloy Hamiltonian is then specified by

$$H=p^2/2m+\textstyle\sum_l V_l,\quad V_l=V_l^{Si}\ \text{ or }\ V_l^{Ge} \tag{4.5}$$

with

$$V_l^{Si}=V_l^{vc}+0.63\,\Delta_l\,,\quad V_l^{Ge}=V_l^{vc}-0.37\,\Delta_l\,, \tag{4.6}$$

and Δ_l given by Eqs. (3.4) and (4.2)–(4.4).

Because of the sharp cutoff in their Fourier components defined by (4.2), it will be observed that the kets $|wl\rangle$ are not really completely cell localized but instead exhibit oscillating behavior at large r. This lack of localization has, however, a negligible effect on the properties of SiGe within the CPA, because according to Eq. (3.7), in which all the parameters characterizing the band structure are defined, the higher components $\phi(\vec{k}+\vec{K})$ appear in the CPA only as factors of the corresponding coefficients $a_{n\vec{K}}(\vec{k})$ of the pseudo-wave-functions, and these are small in SiGe for $|\vec{k}+\vec{K}|$ near k_{max}.

In principle, one could now proceed to solve the CP equations for $F(z)$ and $g(z)$ and then compute the various properties of the alloy directly. However, the calculation of $F(z)$ from (3.5) and also $\rho(E)$ from (3.9) would be a formidable task involving sums over the Brillouin zone of partial

derivatives of the rapidly varying function

$$\mathfrak{L}_{\vec{k}}(g,z)=\ln[1-gQ_1(\vec{k},z)+g^2Q_2(\vec{k},z)]\ . \tag{4.7}$$

We have therefore simplified the calculation of F and ρ in SiGe by applying to $\mathfrak{L}_{\vec{k}}$ two approximations, motivated purely by calculational convenience. The first is to take

$$\begin{aligned}\mathfrak{L}_{\vec{k}}(g,z)&=\ln\Big[1-g\sum_n f_{n\vec{k}}/(z-E_{n\vec{k}})\\&\quad+g^2\sum_{nn'}f_{nn'\vec{k}}/[(z-E_{n\vec{k}})(z-E_{n'\vec{k}})]\Big]\\&\sim\sum_n\ln[1-gf_{n\vec{k}}(z-E_{n\vec{k}})^{-1}]\ ,\end{aligned} \tag{4.8}$$

where $f_{n\vec{k}}=f^C_{n\vec{k}}+f^S_{n\vec{k}}$ and

$$f_{nn'\vec{k}}=f^C_{n\vec{k}}f^S_{n'\vec{k}}-[f^C_{n\vec{k}}f^S_{n\vec{k}}f^S_{n'\vec{k}}f^C_{n'\vec{k}}]^{1/2}\ ,$$

$f^C_{n\vec{k}}$ and $f^S_{n\vec{k}}$ being defined by Eq. (3.7). This approximation amounts to a neglect of all factors involving two or more different bands in an expansion of (4.7) in a Taylor series. It tends to be valid when the broadening of the various bands is much smaller than their separation at any given k, and thus amounts to a weak-scattering approximation, which is, however, very well satisfied in SiGe for all z and k.

The second approximation consists of the assumption that

$$f_{n\vec{k}}=f(E_{n\vec{k}})\ , \tag{4.9}$$

i.e., that the weights $f_{n\vec{k}}$ of all states having the same energy are equal. This "isotropy" approximation is good for SiGe over most of the valence band, but probably less so for much of the conduction band. But, since $F(z)$ turns out to be very close to its virtual-crystal value anyway, the calculated broadening of states in the conduction band will probably still be quite accurate.

With assumptions (4.8) and (4.9), expressions (3.5) and (3.9) can be converted into easily evaluated integral representations

$$F(z)=\int_{-\infty}^{\infty}\frac{\rho^w_{vc}(E')}{z-E'-g(z)f(E')}\,dE' \tag{4.10}$$

and

$$\rho(E)=-\pi^{-1}\,\mathrm{Im}\int_{-\infty}^{\infty}\frac{\rho_{vc}(E')}{E^+-E'-g(E^+)f(E')}\,dE'\ , \tag{4.11}$$

where

$$\rho_{vc}(E)=N^{-1}\sum_{n\vec{k}}\delta(E-E_{n\vec{k}}) \tag{4.12}$$

and

$$\rho^w_{vc}(E)=N^{-1}\sum_{n\vec{k}}f_{n\vec{k}}\,\delta(E-E_{n\vec{k}}) \tag{4.13}$$

are the virtual-crystal density of states and the virtual-crystal density of states in orbital $|w0\rangle$, respectively, and

$$f(E')=\rho^w_{vc}(E')/\rho_{vc}(E')$$

is given by Eq. (4.9).

To find the properties of SiGe within the CPA, Eqs. (4.11) and (2.24) have been solved iteratively for $F(E)$ and $g(E)$, with the starting value $g(E)=0$. This required that $\rho^w_{vc}(E)$ be computed with some precision. In this calculation it has been obtained as a histogram consisting of one bar for every 0.005 Ry of energy, with eigenvalues $E_{n\vec{k}}$ and weights $f_{n\vec{k}}$ obtained by accurate diagonalization of H^{vc} on a cubic mesh of k points of density $1/(2\pi/8a)^3$, and interpolated by means of a variant of $\vec{k}\cdot\vec{p}$ perturbation theory on a mesh 1000 times as dense.[7] The average histogram bar should embody statistical fluctuations of no more than 3%. Such fluctuations have all been smoothed by hand in the figures presented in this paper.

The iterative solution for F and g was complicated to a minor degree by the fact that Eq. (2.24) is nominally a quadratic equation in g. But since $g(z)$, being a matrix element of the self-energy operator Σ, is analytic in both half-planes, the correct solution for g can always be picked out as belonging to that branch which remains finite in the limit $|E|\to\infty$.

Once $g(E)$ was known, the alloy density of states was calculated from Eq. (4.9). Spectral functions were obtained directly from Eq. (3.8).

The complex $E_n(\vec{k})$ relations were found by first-order perturbation theory, with the complex eigenvalue $z_{n\vec{k}}$ given by

$$\begin{aligned}z_{n\vec{k}}&\sim E_{n\vec{k}}+\langle n\vec{k}|\,[H_{eff}(z_{n\vec{k}})-H^{vc}]\,|n\vec{k}\rangle\\&=E_{n\vec{k}}+f_{n\vec{k}}g(z_{n\vec{k}})\ .\end{aligned} \tag{4.14}$$

Equation (4.14) is an implicit equation for $z_{n\vec{k}}$. Expanding $g(z_{n\vec{k}})$ in a Taylor series about $E_{n\vec{k}}$, we get to lowest order

$$z^{(1)}_{n\vec{k}}\sim E_{n\vec{k}}+f_{n\vec{k}}g(E_{n\vec{k}})\ , \tag{4.15}$$

or to second order

$$z^{(2)}_{n\vec{k}}\sim E_{n\vec{k}}+f_{n\vec{k}}g(E_{n\vec{k}})/[1-f_{n\vec{k}}dg(E_{n\vec{k}})/dz]\ . \tag{4.16}$$

Expression (4.14) is expected to be a good approximation in SiGe, where the "scattering strength"

$$f_{n\vec{k}}g(E_{n\vec{k}})\sim f_{n\vec{k}}\,\delta\sim\delta\phi_0^2\sim 0.02\ \mathrm{Ry}$$

is much less than the typical separation between bands. The "complex bands" to be exhibited here are based on Eq. (4.15), for two reasons. First, for most values of k, this simple approximation yields about the same degree of accuracy as the explicit diagonalization of H_{eff}. Second, in those

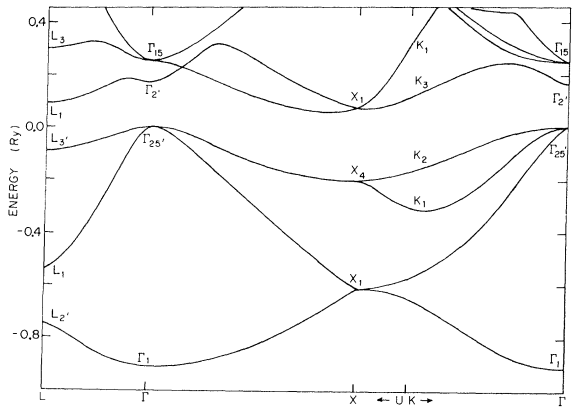

FIG. 1. Band structure of $Si_{0.37}Ge_{0.63}$, virtual-crystal approximation.

few cases where (4.15) is inaccurate the corresponding spectral line usually proves to be so asymmetrical that *no* single complex pole can properly represent it. Note, however, that (4.15)

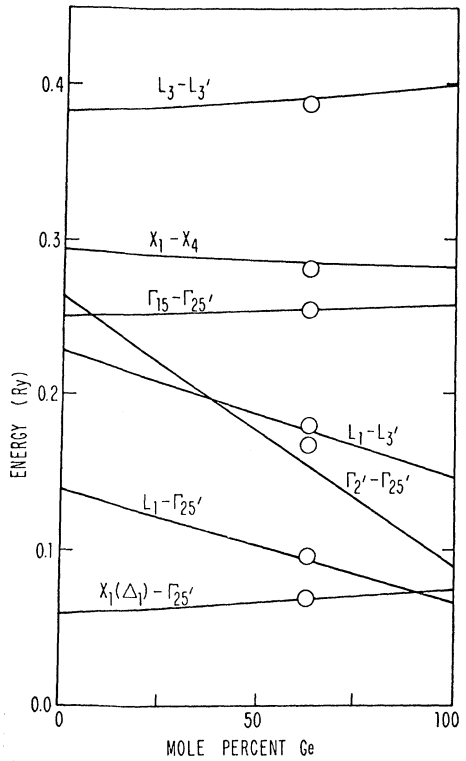

FIG. 2. Virtual-crystal band gaps for SiGe. The straight lines represent a linear interpolation between the results obtained by Brust (Ref. 5) and Si and Ge on the basis of local energy-independent pseudopotential approximation. The dots are values calculated by the authors for $Si_{0.37}Ge_{0.63}$. The radius of the circles is the estimated error in the eigenvalue calculation.

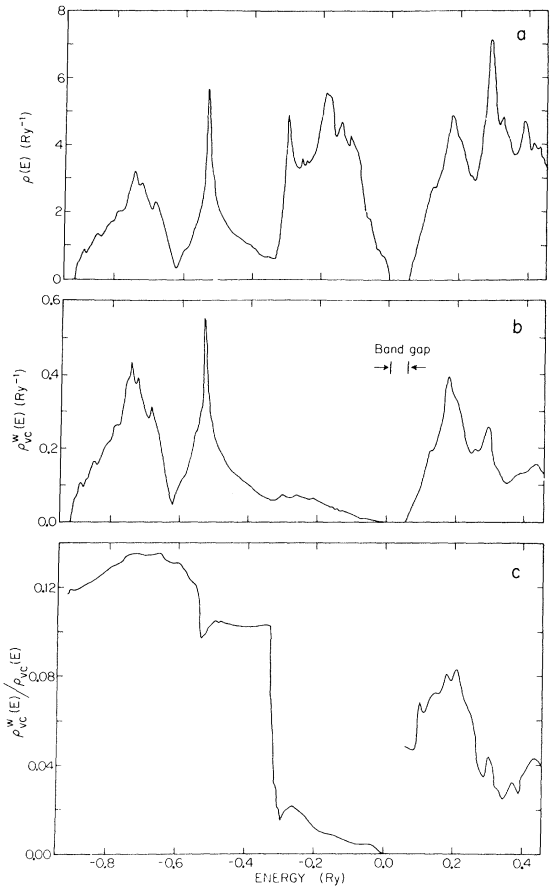

FIG. 3. (a) Density of states per spin polarization of $Si_{0.37}Ge_{0.63}$ virtual-crystal approximation; (b) the density of states for electrons in orbital $|wl\rangle$, virtual-crystal approximation; (c) average weight per state [the ratio of (b) to (a)].

is *not* simply perturbation theory about the virtual crystal, because $g(E)$ is obtained from the self-consistency condition (2.24).

We turn now to a detailed presentation of the results. The band structure of $Si_{0.37}Ge_{0.63}$ in the virtual-crystal approximation is shown in Fig. 1. The bands, not surprisingly, correspond to almost a linear interpolation of the pure Si and Ge bands calculated on the basis of the Brust form factors. This is shown more explicitly in Fig. 2, where various virtual-crystal band gaps may be seen to be nearly on a line between the pure crystal band gaps. The principal exception to this rule is the gap involving $\Gamma_{2'}$, which also turns out to be the state most broadened by alloy scattering.

Additional properties of the virtual crystal are shown in Fig. 3. The density of states $\rho_{vc}(E)$ shown in Fig. 3(a) is notable for a sharp peak at about -0.52 Ry, which arises from states on or

just beneath the hexagonal faces of the Brillouin zone. The other peaks do not originate from any localized portion of the zone. The weighted density of states

$$\rho_{vc}^{w}(E) = -\pi^{-1}\,\mathrm{Im}\langle w0|\,(E^{+}-H^{vc})^{-1}\,|w0\rangle$$

[Fig. 3(b)] retains qualitatively most of the features of Fig. 4(a), with the striking exception of the broad peak at the top of the valence band, which is almost entirely absent. Its absence is reflected in Fig. 3(a), where the function $f(E)=\rho_{vc}(E)/\rho_{vc}^{w}(E)$ is evidently much smaller near the top of the valence band than elsewhere.

The behavior in Figs. 3(b) and 3(c) may be explained as follows. Because of assumption (4.2), the weight $f_{n\vec{k}}=|\langle n\vec{k}|w0\rangle|^2$ represents the overlap of a Bloch state with a spherically symmetrical orbital, and will be appreciable only for virtual-crystal states with substantial s-like character. The function

$$\rho_{vc}^{w}(E)=\sum_{n\vec{k}} f_{n\vec{k}}\,\delta(E-E_{n\vec{k}})$$

is thus a measure of that character in states of energy E. Electrons near the top of the valence band, being mostly p-like, will contribute very little to this function in contrast to states elsewhere in the valence band. This is particularly clear at the point Γ, where the four valence states consist of one pure s and three degenerate p states, lying, respectively, at the bottom and the top of the valence bands. Similarly, the existence of many s-like states in the conduction band, especially near $\Gamma_{2'}$, is reflected in a large peak in $f(E)$ near 0.2 Ry. Indeed, $f_{n\vec{k}}$ for $\Gamma_{2'}$ itself is 0.41, the largest of any state in either the valence or the conduction band. Nevertheless, the magnitude of the associated peak in $\rho_{vc}^{w}(E)$ is lessened by the fact that such strongly s-like states coexist with many others of similar energies which have very little s character.

Figure 4 shows the matrix element $g(E)$ of the self-energy operator Σ in $Si_{0.37}Ge_{0.63}$. $\mathrm{Im}g(E)$ resembles in shape the curve for $\rho_{vc}^{w}(E)$ [Fig. 3(b)], which acts somewhat like an effective density of available states for scattering. The relation $\mathrm{Im}g(E)\propto\rho_{vc}^{w}(E)$ which is qualitatively exhibited in Figs. 3 and 4 is characteristic of the virtual-crystal regime, where $|\delta F|\ll 1$: Expanding Eq. (2.24) in powers of δF yields

$$g(E)\sim x(1-x)\,\delta^2 F\,, \tag{4.17}$$

or, to lowest order in $|\delta F_0|$,

$$g\sim x(1-x)\,\delta^2 F_0\,,$$

i.e.,

$$\mathrm{Im}g\sim\pi x(1-x)\delta^2\rho_{vc}^{w}\,. \tag{4.18}$$

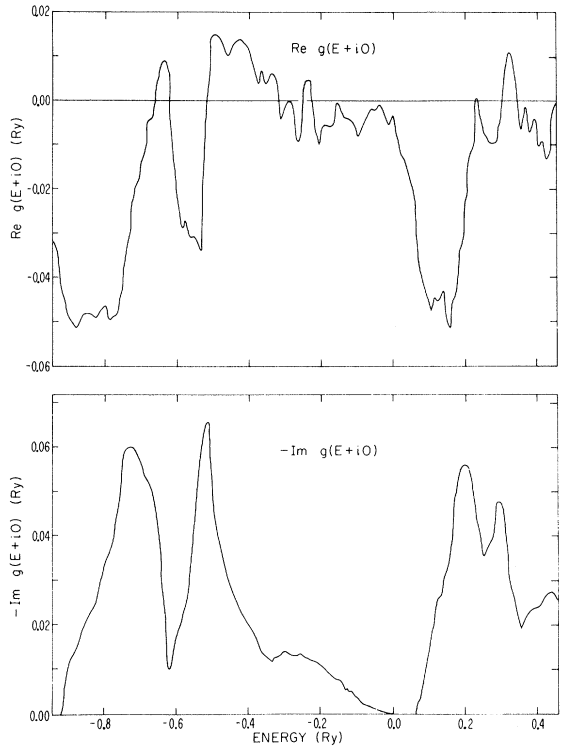

FIG. 4. Real and imaginary parts of $g(E+i0)$, $Si_{0.37}Ge_{0.63}$.

However, in $Si_{0.37}Ge_{0.63}$, $\mathrm{Im}g(E)$ deviates from (4.18) by as much as 20%. The deviations are largest where g is itself largest. This discrepancy indicates that effects due to alloy scattering are not always given accurately by low-order perturbation theory about the virtual crystal. [It should be noted, however, that the deviation in Fig. 4 may not have been accurately calculated in the conduction band because of the isotropy approximation (4.9)].

The self-energy $\Sigma_{n\vec{k}}(E)$ of an electron in virtual-crystal state $|n\vec{k}\rangle$ is not given by $g(E)$, but instead by a more complicated $\vec{k}$-dependent expression which we shall not give explicitly for the diamond lattice. For the weak-scattering alloy SiGe, where the broadening of the bands is much smaller than their separation, $\Sigma_{n\vec{k}}(E)$ is accurately given by

$$\Sigma_{n\vec{k}}(E)\sim g(E)f_{n\vec{k}}\,. \tag{4.19}$$

Thus, in addition to the effective energy-dependent scattering potential $g(E)$, there is a $\vec{k}$-dependent matrix element $f_{n\vec{k}}$ which determines to what extent an electron in state $|n\vec{k}\rangle$ "feels" the potential, and which, thus, helps determine the broadening of the state.

Figure 5 presents the density of states of $Si_{0.37}$

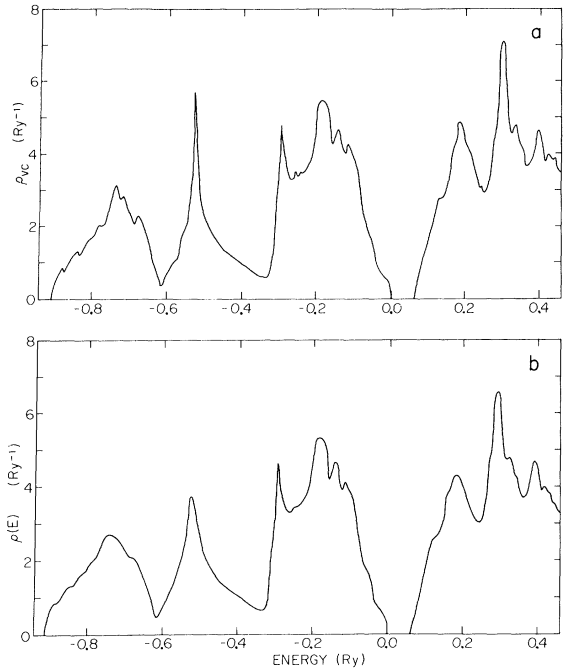

FIG. 5. (a) Virtual-crystal density of states per spin polarization in $Si_{0.37}Ge_{0.63}$; (b) the same in the coherent potential approximation.

$Ge_{0.63}$ in the CPA, along with the virtual-crystal density of states, shown for the purpose of comparison. $\rho(E)$ differs from ρ_{vc} principally in the lower half of the valence band, where the peaks of the former are somewhat lower and broader and exhibit less fine structure. Some damping is also evident in the conduction band. But throughout the interval of 0.3 Ry immediately below the valence-band maximum, the electron states are mostly p-like and, as a result, the broad peaks occurring at those energies in ρ_{vc} are substantially unchanged in the alloy.

In order to illustrate how much more the disorder may affect one part of the density-of-states curve than another, we have carried out additional calculations on two fictitious alloys $A_{0.37}B_{0.63}$ having atomic pseudopotentials (4.6), but with $\delta = 1.02$ and 2.04 Ry, exactly twice and four times its value in SiGe. The densities of states for these two alloys are shown in Fig. 6. As δ increases, the s-like peaks in the lower half of the valence bands are shifted to lower energies and are almost entirely flattened out, whereas the broad p-like peak at the top of the band remains almost unchanged. The conduction-band peaks undergo an intermediate degree of change. Because of the approximations made in carrying out the calculation, only qualitative significance should be attributed to these curves.

For all four of the alloys shown in Figs. 5 and 6, the total number of valence states per atom per spin polarization remains 2.0 within computational accuracy of 1%, reflecting the fact that even for the largest δ considered the spectral function

$$A_n(\vec{k}, E) = -\pi^{-1}\langle n\vec{k}|\,\overline{G}(E^+)\,|n\vec{k}\rangle$$

associated with a valence state $|n\vec{k}\rangle$ has negligible density in the conduction band.

The remaining three figures depict some of the $\vec{k}$-dependent properties of $Si_{0.37}Ge_{0.63}$. The spectral function $A(\vec{k}, E)$ is shown in Fig. 7 for three points of high symmetry in the Brillouin zone. The various spectral lines are all narrow compared to the bandwidth and are for the most part Lorentzian in shape, indicating that they are well approximated by complex band energies. Notable exceptions are the states Γ_1 and $\Gamma_{2'}$ with which the CPA associates narrow but asymmetrical spectral lines. Such asymmetries are largely, but not entirely, due to the sharp band edges (i.e., infinite $d\rho/dE$) which the CPA requires at all energies where the density of states goes to zero. Since all spectral functions must be zero where there is no density of states, the Lorentzian tail in states like Γ_1 and $\Gamma_{2'}$ is prematurely truncated on the low-energy side. As has been pointed out by Lifshitz,[17] the existence of large clusters of like atoms in a disordered binary alloy for statistical reasons results in the existence of an ex-

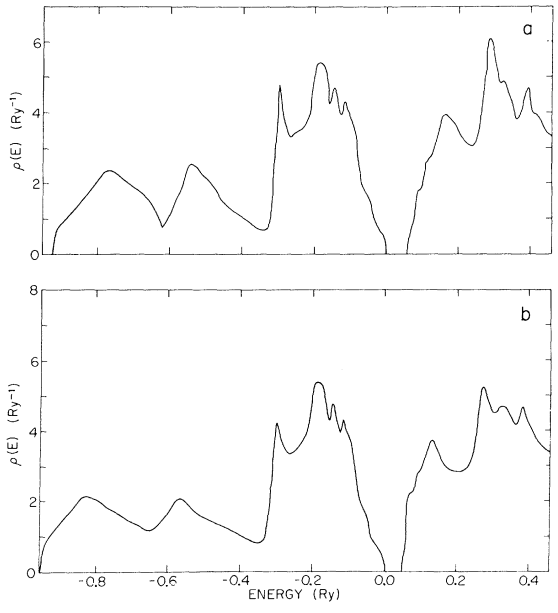

FIG. 6. Density of states for two fictitious alloys $A_{0.37}B_{0.63}$ having atomic pseudopotentials given by (4.6) and (2.22), with (a) $\delta = 1.02$; (b) $\delta = 2.04$.

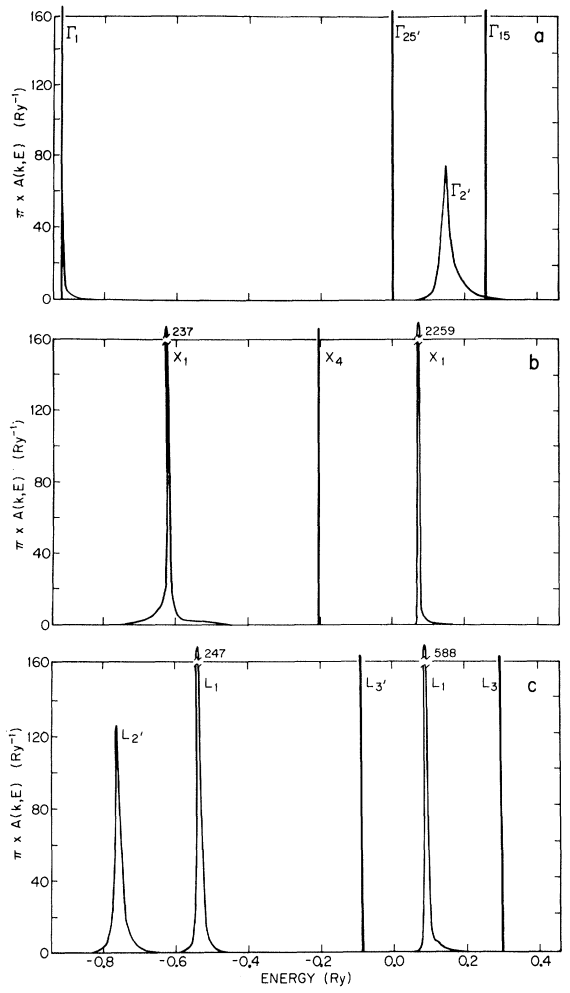

FIG. 7. Spectral density $A(\vec{k}, E)$ [Eq. (2.11)] for three points of high symmetry in the Brillouin zone: (a) $\Gamma = 2\pi/a\,(0,0,0)$; (b) $X = 2\pi/a\,(1,0,0)$; (c) $L = 2\pi/a\,(\frac{1}{2},\frac{1}{2},\frac{1}{2})$. The numbers near several of the peaks denote the maximum heights of the adjacent peaks; the heavy vertical lines represent energies where the spectral function is infinite.

ponentially diminishing tail in the density of states and spectral functions at band edges. In SiGe this would presumably reduce (though not eliminate) the asymmetry of such spectral lines.

The complex band structure of the alloy is presented in Fig. 8. The states most significantly broadened lie in the s-like conduction band near $\Gamma_{2'}$. Note that the other states at approximately the same energy are hardly broadened at all. The reasons for this behavior may be understood from Fig. 9 which shows the virtual-crystal bands and their weights $f_{n\vec{k}}$, and from Fig. 4(b) which exhibits the imaginary part of the effective potential $g(E)$. The alloy bands of Fig. 8, which are derived from Eq. (4.15), have half-width given by

$$2\,\mathrm{Im}z_{n\vec{k}} = 2f_{n\vec{k}}\,\mathrm{Im}g(E_{n\vec{k}})\ . \tag{4.20}$$

The broadenings of Fig. 8, small as they are, deviate by as much as 20% from the values predicted by low-order perturbation theory. These latter, to lowest order in δF, are given by

$$2\,\mathrm{Im}z_{n\vec{k}} = 2x(1-x)\delta^2\,\mathrm{Im}F(E_{n\vec{k}}) \tag{4.21}$$

upon using Eqs. (4.15) and (4.17). The greatest differences between the CPA and perturbation theory occur at $\Gamma_{2'}$, where the broadening is itself greatest.

We do not expect that the departure of SiGe from virtual-crystal behavior, as shown principally in Figs. 5, 7, and 8, will have substantial effect on the interband optical properties or the electrical properties of the alloy. Those states most substantially broadened – the ones in the s band near $\Gamma_{2'}$ – appear in the absorption spectrum superimposed upon other absorption peaks arising from states near the bottom of the conduction band, and are greatly masked. The shifts in the band energies due to disorder scattering – i.e., the values of $\mathrm{Re}(z_{n\vec{k}} - E_{n\vec{k}})$ – are also very small, and the generally linear behavior of the virtual-crystal band gaps should persist in the alloy. Clustering-induced tailing of the conduction-band edge does not appear in the CPA, but neither is it visible on any of the published experimental curves.[8,9,16,18,19]

The effect of disorder scattering on the static electrical properties of SiGe, where the scattering is weak and isotropic, can be well accounted for by a single-particle relaxation-time approximation.[20] We find that for n-type $Si_{0.37}Ge_{0.63}$ the Hall mobility at room temperature should be $\mu_H^{\mathrm{alloy}} \sim 10^5\ \mathrm{cm^2/V\,sec}$, about 50 times greater than the observed value, which is thus determined at that temperature principally by phonon or ionized impurity scattering. μ_H^{alloy} varies with temperature like $T^{-1/2}$ as is characteristic of neutral impurity scattering. μ_H^{alloy} for p-type SiGe turns out to be infinite. The reason for this behavior is that the holes at the top of the valence band are purely p-like and never experience the lattice disorder, which is concentrated in the ionic cores and affects only s states.

The insensitivity of the experimental parameters in SiGe to alloy disorder is hardly surprising in an alloy in which the strong random atomic potentials can be replaced by weak random pseudopotentials, and in which, furthermore, the difference between the potentials is concentrated in the ionic cores from which most of the valence electrons are largely excluded. However, the calculations described here provide the most detailed theoretical evidence presented thus far for the validity of the virtual-crystal model for SiGe al-

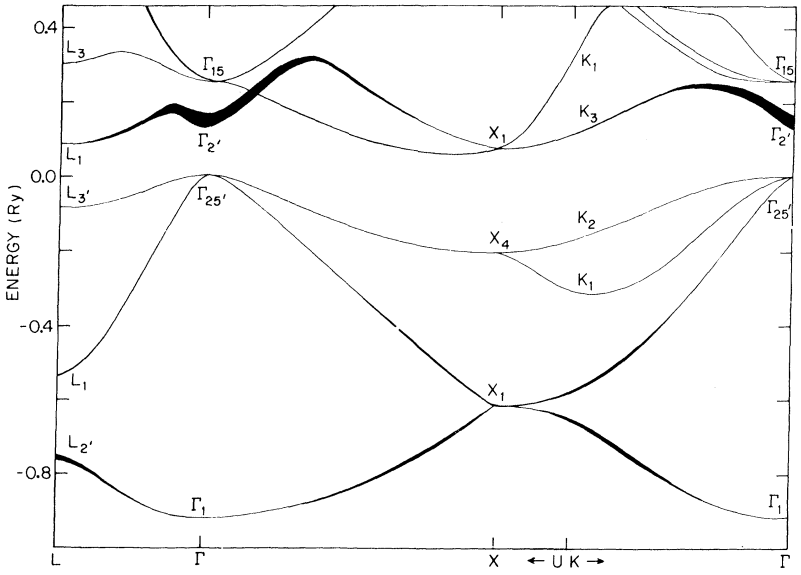

FIG. 8. Complex $E_n(\vec{k})$ relations for $Si_{0.37}Ge_{0.63}$, as derived from Eq. (4.15). The half-width of a shaded line represents twice the imaginary part of the associated complex eigenvalue.

loys even though its correctness has been long recognized on the basis of experimental information. More importantly, the present work provides a framework which may be useful for calculations pertaining to other alloy systems in which the virtual-crystal approximation is not as appropriate.

ACKNOWLEDGMENTS

We are grateful to B. Velický for a number of useful discussions. Helpful comments from S. Kirkpatrick and L. Schwartz are also appreciated.

Note added in proof. M. Cardona has kindly called to our attention the results of electroreflectance experiments carried out on disordered SiGe alloys [J. S. Kline, F. H. Pollak, and M. Cardona, Helv. Phys. Acta 41, 968 (1968)] of which we were not previously aware. These experiments seem to suggest that the width of the state Γ_2' is substantially smaller than that obtained in the present calculations. We wish to point out two possible reasons for this seeming discrepancy. First, the calculated widths are extremely sensitive to the exact choice of the Si and Ge model potentials. A reduction of only 0.01 Ry in the differences between the Si and Ge form factors, for example, would reduce the broadenings by a factor of 4 according to second-order perturbation theory [Eq. (4.21)], and probably by a similar amount in the CPA.

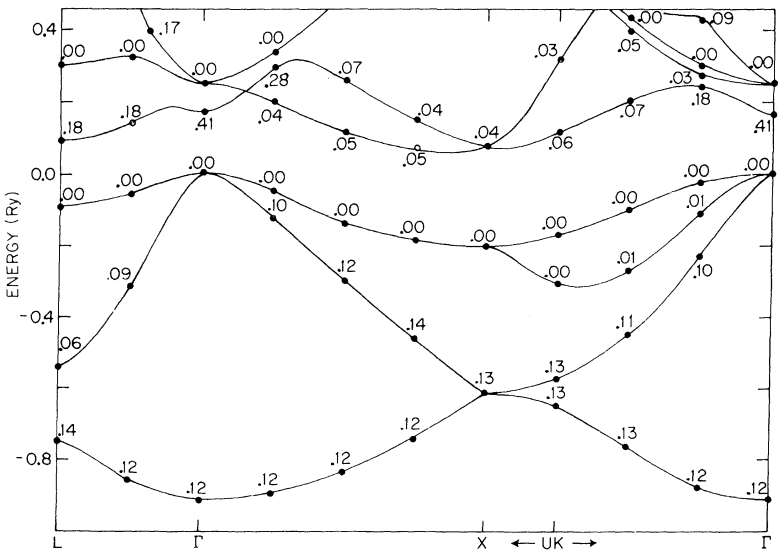

FIG. 9. Virtual-crystal band structure, $Si_{0.37}Ge_{0.63}$. The numbers near the various band energies E_{nk} represent the corresponding weights $f_{n\vec{k}}$.

Second, the present work does not take account of effects arising from the nonlocal character of the pseudopotential. In the (nonlocal) Heine-Abarenkov approximation [V. Heine and I. Abarenkov, Phil. Mag. 9, 451 (1964)], the Si and Ge pseudopotentials differ principally in their scattering of d waves [A. O. E. Animalu and V. Heine, Phil. Mag. 12, 1249 (1965)], not s waves as in the present model. This presumably reflects the fact that the Ge ion has a filled d shell, which the Si ion lacks. However, as in the present model, the Heine-Abarenkov pseudopotential is the same for Si and Ge ions outside a certain core radius.

Since it is not obvious how these various effects would modify the observed broadenings in Si_xGe_{1-x}, our numerical results should be considered in the spirit of a pilot calculation. It should be emphasized, however, that the present formalism may readily be generalized to more realistic nonlocal pseudopotential models from which band broadenings could be more accurately calculated.

We are grateful to M. Cardona, J. C. Phillips, and B. O. Seraphin for enlightening discussions of these questions.

*Supported in part by Grant No. GP-8019 of the National Science Foundation and the Advanced Research Projects Agency.

†Present address: Laboratory of Atomic and Solid State Physics, Clark Hall, Cornell University, Ithaca, N. Y. 14850.

[1]P. Soven, Phys. Rev. 156, 809 (1967).
[2]D. W. Taylor, Phys. Rev. 156, 1017 (1967).
[3]Y. Onodera and Y. Toyozawa, J. Phys. Soc. Japan 24, 341 (1968).
[4]B. Velický, S. Kirkpatrick, and H. Ehrenreich, Phys. Rev. 175, 747 (1968).
[5]P. Soven, Phys. Rev. 178, 1136 (1969).
[6]S. Kirkpatrick, B. Velický, and H. Ehrenreich, Phys. Rev. (to be published).
[7]A detailed discussion of the numerical methods and approximations used is to be found in D. Stroud, Ph. D. dissertation, Harvard University, 1969 (unpublished).
[8]F. Herman, Phys. Rev. 95, 847 (1954).
[9]J. Tauc and H. Abraham, J. Phys. Chem. Solids 20, 190 (1961).
[10]F. Bassani and D. Brust, Phys. Rev. 131, 1524 (1963).
[11]See, for example, P. Nozières, *Theory of Interacting Fermi Systems* (Benjamin, New York, 1963), pp. 345–51.
[12]B. J. Austin, V. Heine, and L. J. Sham, Phys. Rev. 127, 276 (1962).
[13]P. Lloyd, Proc. Phys. Soc. (London) 90, 207 (1967).
[14]Yu. A. Izyumov, Advan. Phys. 14, 569 (1965).
[15]D. Brust, Phys. Rev. 134, A1337 (1964).
[16]E. Schmidt, Phys. Status Solidi 27, 57 (1968).
[17]I. M. Lifshitz, Usp. Fiz. Nauk. USSR 83, 617 (1964) [Soviet Phys. Usp. 7, 549 (1965)].
[18]E. R. Johnson and S. M. Christian, Phys. Rev. 95, 560 (1954).
[19]R. Braunstein, A. R. Moore, and F. Herman, Phys. Rev. 109, 695 (1958).
[20]B. Velický, Phys. Rev. (to be published).

PHYSICAL REVIEW B VOLUME 2, NUMBER 8 15 OCTOBER 1970

Anistropy of the Constant-Energy Surfaces in n-Type Bi_2Te_3 and Bi_2Se_3 from Galvanomagnetic Coefficients*

L. P. Caywood, Jr.,† and G. R. Miller
University of Utah, Salt Lake City, Utah 84112
(Received 17 November 1969)

Low-field galvanomagnetic coefficients have been measured on single crystals of Bi_2Te_3 and Bi_2Se_3 at 76 °K in fields to 9 kG. Using a six-valley ellipsoid model in the isotropic relaxation-time approximation, the mass parameters of the ellipsoids are calculated for both compounds. The discrepancy between previously reported galvanomagnetic data and de Haas–van Alphen data for Bi_2Te_3 can be minimized by recalculating the mass parameters from the galvanomagnetic data and by not assuming complete degeneracy. The experimental data on Bi_2Te_3 are in agreement with those reported earlier. There is also very good evidence of second-band effects at high electron concentrations ($> 10^{19}$ cm^{-3}), as has been previously suggested. The constant-energy surfaces undergo an apparent change in shape between low- and high-concentration samples. Data on Bi_2Se_3 indicate that the constant-energy surfaces are more spherical than in the case of Bi_2Te_3.

I. INTRODUCTION

Because of their possible application in efficient thermoelectric devices, the intermetallic compounds Bi_2Te_3 and Bi_2Se_3 and their alloys have received a great deal of attention in the last decade. An extensive literature is available and several review